A Multi-Parameter Analysis of Cellular Coordination of Major Transcriptome Regulation Mechanisms

Wen Jiang[a,b], Zhanyong Guo[d], Nuno Lages[e], W. Jim Zheng[f], Denis Feliers[g], Fangyuan Zhang[c], Degeng Wang[a,b,h]

[a]Department of Environmental Toxicology, [b]The Institute of Environmental and Human Health (TIEHH), [c]Department of Mathematics & Statistics, Texas Tech University, Lubbock, TX 79409.

[d]National Key Laboratory of Wheat and Maize Crop Science, College of Agronomy, Henan Agricultural University, Zhengzhou, Henan 450002, P. R. China

[e]Instituto Superior Técnico, Universidade de Lisboa, IST-Taguspark, 2744-016 Porto Salvo, Portugal

[f]School of Biomedical Informatics, The University of Texas Health Science Center at Houston, 7000 Fannin Street, Suite 600, Houston, TX 77030.

[g]Department of Medicine/Renal Diseases, The University of Texas Health Science Center at San Antonio, San Antonio, TX

[h]: Corresponding author. Email: degeng.wang@ttu.edu.

Keywords: multi-parameter analysis, polysome, post-transcription regulation, transcription rate (TR), untranslated region (UTR)

Abstract

To understand cellular coordination of multiple transcriptome regulation mechanisms, we simultaneously measured three parameters – transcription rate (TR), mRNA abundance (RA) and translation activity (TA) – and assessed mRNA stability with the RA to TR ratio. This revealed multiple quantitative insights. First, the dataset enabled an assessment of the contribution of the stabilization-by-translation regulatory mechanism. We observed an overall positive correlation between mRNA stability and translation activity. However, the correlation is moderate. Many genes deviate from the overall trend in a pathway/function specific manner. Second, the moderateness of this correlation can be explained by variation in individual mRNAs' proportions occupied by un-translated regions (UTR), as the UTR proportion exhibits a negative relationship with the level of correlation between the two factors. High-UTR-proportion mRNAs largely defy the stabilization-by-translation regulatory mechanism, in that they stay out of the polysome complex but remain relatively stable; mRNAs with little UTRs, on the contrary, follow this regulation much better. Third, the genomic profiles of the three parameters are systematically different in terms of key statistical features. Sequentially more genes exhibit extreme low or high expression values from TR to RA, and then to TA. In other words, as a consequence of the cellular activities in coordinating these regulatory mechanisms, sequentially higher levels of selectivity are imposed on the gene expression process as genetic information flow from the genome to the proteome. In summary, we presented a quantitative delineation of the relationship among multiple transcriptome regulation parameters, *i.e.*, how the cells coordinate corresponding regulatory mechanisms.

Introduction

The genomic sequences are readily available for a large and ever-increasing number of species. These sequences, like English literature, represent static strings of symbols/alphabets (A, T, C, and G). Hence, genomic sequences are often termed as the "book" of life. To some degree, the cell can be considered as the "reader" of the genomic "book", and the multi-stepped gene expression process as the "reading" process (Searls 1997, Searls 2001, Searls 2002, Wang 2005). Through the gene expression process, the seemingly simplistic genomic alphabetical strings are selectively and dynamically transcribed into transcriptome sequences, which are in turn translated into amino acid sequences in the proteome – the main machinery that controls biochemical reactions and processes in support of cellular functions. This process is integral to essentially all cellular activity. Lately, the complexity of this process has been the target of intensive investigative efforts (Schwanhausser, Busse et al. 2011, Vogel and Marcotte 2012, Li, Bickel et al. 2014, Rabani, Raychowdhury et al. 2014, Jovanovic, Rooney et al. 2015, McManus, Cheng et al. 2015, Liu and Aebersold 2016).

The transcriptome and the proteome have long been routinely measured with high-throughput technologies, currently primarily in the form of mRNA and protein abundance. Perhaps due to the availability of more powerful technologies, transcriptome analysis is more prevalent than proteome analysis. The next generation sequencing (NGS) techniques have gradually become the technique of choice to measure mRNA abundance, due to their ultra-high throughput, scalability, relatively good data quality and repeatability. Essentially all expressed transcript can be reliably and quantitatively detected. Proteomic analysis, on the other hand, does not have a technology that is nearly as effective. Mass spectrometry, arguably the most widely used proteomic technology, has the power to reliably detect thousands of proteins in human cells. Many expressed proteins are missed. Nevertheless, proteins are the direct executers and/or regulators of most biochemical reactions, and therefore, proteomic analysis is of great biomedical importance.

In some experiments, mRNA and protein abundance are measurs simultaneously. One lesson we learned is that correlation between the two is not always satisfactory enough for mRNA abundance to be a reliable predictor of protein abundance. This discrepancy had been observed prior to the genomic era (Anderson and Seilhamer 1997, Gygi, Rochon et al. 1999). It was confirmed in the yeast *S. cerevisiae* by

one of the first simultaneous transcriptome and proteomic measurement (Ideker, Thorsson et al. 2001), and then observed in many other high-throughput studies (Griffin, Gygi et al. 2002, Ghaemmaghami, Huh et al. 2003, Washburn, Koller et al. 2003, Le Roch, Johnson et al. 2004, Tian, Stepaniants et al. 2004, Flory, Lee et al. 2006, Schwanhausser, Busse et al. 2011, Jovanovic, Rooney et al. 2015, McManus, Cheng et al. 2015, Cheng, Teo et al. 2016).

Transcriptome analysis techniques have also been coupled to conventional experimental protocols to measure other gene expression parameters. Initially micro-array (Garcia-Martinez, Aranda et al. 2004, Molina-Navarro, Castells-Roca et al. 2008, Romero-Santacreu, Moreno et al. 2009, Marin-Navarro, Jauhiainen et al. 2011), and then NGS (Core, Waterfall et al. 2008, Hah, Danko et al. 2011), were coupled to the nuclear run-on technique for genome-wide transcription rate measurement. Additionally, NGS was coupled to metabolic labeling of nascent transcripts to measure transcription rate (Dolken, Ruzsics et al. 2008, Friedel, Dolken et al. 2009, Rabani, Levin et al. 2011, Schwanhausser, Busse et al. 2011, Eser, Demel et al. 2014). These strategies enabled simultaneous transcription rate and mRNA abundance measurement. Once again, some levels of discrepancy were observed in that mRNA abundance was not always a good predictor of transcription rate.

These observed discrepancies among gene expression parameters were thought as a reflection of the complexity of the gene expression process, (Greenbaum, Colangelo et al. 2003) and should be informative for us to unravel the complexity. At the same time nascent RNA and protein are produced, existing RNA and protein are being selectively degraded. The abundance of protein and mRNA represent the balance of the respective production and degradation. Discrepancy among gene expression parameters is considered evidence for some levels of decoupling among transcription, translation, mRNA degradation and protein degradation; that is, the gene expression parameters can be divergently regulated. Given the technical feasibility, multi-parameter approaches are being used to study the discrepancy and glean out fundamental gene expression regulation principles. Such studies will potentially lead to more efficient gene expression analysis strategies that generate more informative data.

Such multi-parameter approaches should be especially valuable for transcriptome analysis. The ribosome profiling analysis utilizes NGS to quantify polysome-associated mRNAs, i.e., actively

translating mRNAs, thus enabling genome-wide analysis of translation activity (Ingolia, Ghaemmaghami et al. 2009, Brar, Yassour et al. 2012). Thus, all techniques are in place for genome-wide integration of transcription rate (GRO-seq), mRNA abundance (RNA-seq) and mRNA translation activity (ribosome profiling). This will generate an integrative view of the transcriptome and its dynamic regulation, i.e., how the multiple transcriptome regulatory mechanisms are coordinated.

Additionally, such data is needed as a platform to study mRNA untranslated regions (UTR), where the majority of regulatory signals for post-transcriptional regulation are embedded. It is well documented that mRNA UTRs are responsible for mRNA stability and translation control. They contain binding sites for microRNA and many regulatory RNA-binding proteins. They are common in mammalian mRNAs. Human mRNAs, on average, have ~1000 nucleotide long UTRs (~800 nucleotide 3'- and ~200 nucleotide 5'-UTRs). Systematic functional study of the UTRs, however, awaits multi-parameter datasets that enables simultaneous study of mRNA stability and translation activity.

Thus, we generated a multi-parameter snapshot of the transcriptome of a human cell line. Genome-wide transcription rate (TR), mRNA abundance (RA) and translation activity (TA) are simultaneously measured. Briefly, we observed different statistical features of the genomic profiles of the three parameters. We indirectly assessed mRNA stability/degradation by the RA to TR ratio. We also assessed the effect of translation on mRNA degradation, as it is known that actively translating mRNA is protected from degradation (Coldwell, Gray et al. 2010, Morozov, Jones et al. 2012). Even though a general trend of positive correlation between mRNA stability and translation activity was observed, many genes deviate from this general trend in a function-specific manner. Analysis of the data in conjunction with mRNA UTRs revealed insights into, and the roles of UTRs in, cellular coordination of these transcriptome regulatory mechanisms.

Results

Significant discrepancy among the three parameters

Previously, we have analyzed publicly available genomic datasets, in which multiple gene expression parameters are simultaneously measured (Wang 2008, Hayles, Yellaboina et al. 2010). In those studies, we attempted to explain the discrepancy among gene expression parameters, which seemed then mysterious to most scientists, from the perspectives of biochemical pathway/network control and cellular operations. The genome-wide measurement techniques have since greatly advanced, and many datasets have recently been published (Goodwin, McPherson et al. 2016). However, we have not seen a dataset that integrate TR, RA, TA and mRNA stability; the translational data in such studies are mass-spectrometry-based, and thus the coverage is not nearly genome-wide. Thus, in the present work, we took advantage of the genome-wide analysis power of NGS and its versatility through successful coupling to a variety of conventional experimental protocols. Our goal is to simultaneously measure TR, RA and TA, that is, to obtain a genome-wide multi-parameter snapshot of the transcriptome, in the HCT116 human cells. The experimental strategy is illustrated in Figure 1. The experiments were done with cells in exponential growth (log) phase (see Materials and Methods for details). We measured RA with the standard RNA-seq method. Simultaneously, we measured genome-wide TR and TA, using the GRO-seq technique and a protocol similar to the ribosome profiling technique, respectively. The NGS reads were aligned to the human genome with TopHat (Kim, Pertea et al. 2013) and the read counts for expressed genes were calculated with the HTSeq-count software (Anders, Pyl et al. 2015). The read counts were then converted into Reads Per Kilo-base Per Million Mapped Reads (RPKM) values. With a cut-off of 1 RPKM for at least one of the three parameters, 12921 genes were found expressed in the HCT116 cells.

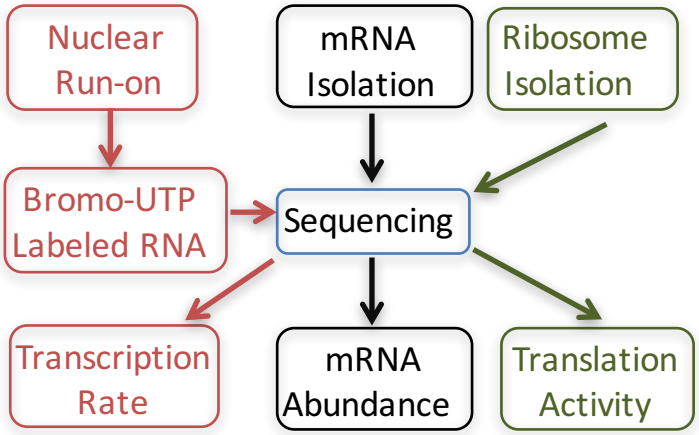

Figure 1: Experimental strategy. Log-phase HCT116 cells were split up into three parts. One part was used to extract total mRNA for RNA-seq analysis to measure steady-state mRNA abundance (RA) (black texts and arrows). One part was used to perform nuclear run-on to generate bromo-UTP labeled nascent RNA for sequencing, that is, GRO-seq analysis to measure transcription rate (TR) (green texts and arrows). The last part was used to isolate and quantify polysome associated mRNA to measure translation activity (TA) (green texts and arrows).

Comparative analysis of the three gene expression parameters revealed extensive difference among them. Individual pairwise comparison resulted in, as expected, a general trend of good correlation; that is, association of a high value of one parameter with high values of other parameters. However, when analyzed together, they revealed quite dramatic differences, which are way beyond intrinsic experimental noises, among the three parameters (Fig. 2). In Figure 2A, TR and one RA biological replicate are plotted against another RA biological replicate, with the two RA replicates illustrating the level of the intrinsic experimental noises. The two RA replicates agree with each other well, with a linear regression slope of about 1 and a low level of dispersion along the regression line. However, the regression of TR versus the RA replicate is dramatically different. The slope of regression line is only 0.44, suggesting systematic difference between the two parameters. Additionally, as shown in Figure 2B, the regression line between RA and TA is also different from that between the two RA replicates. The change in the slope of the regression line, an increase to 1.11, is not as dramatic. But, statistically, it is highly significant, with a p-value of less than 1E-200 – essentially zero (see Materials and Methods

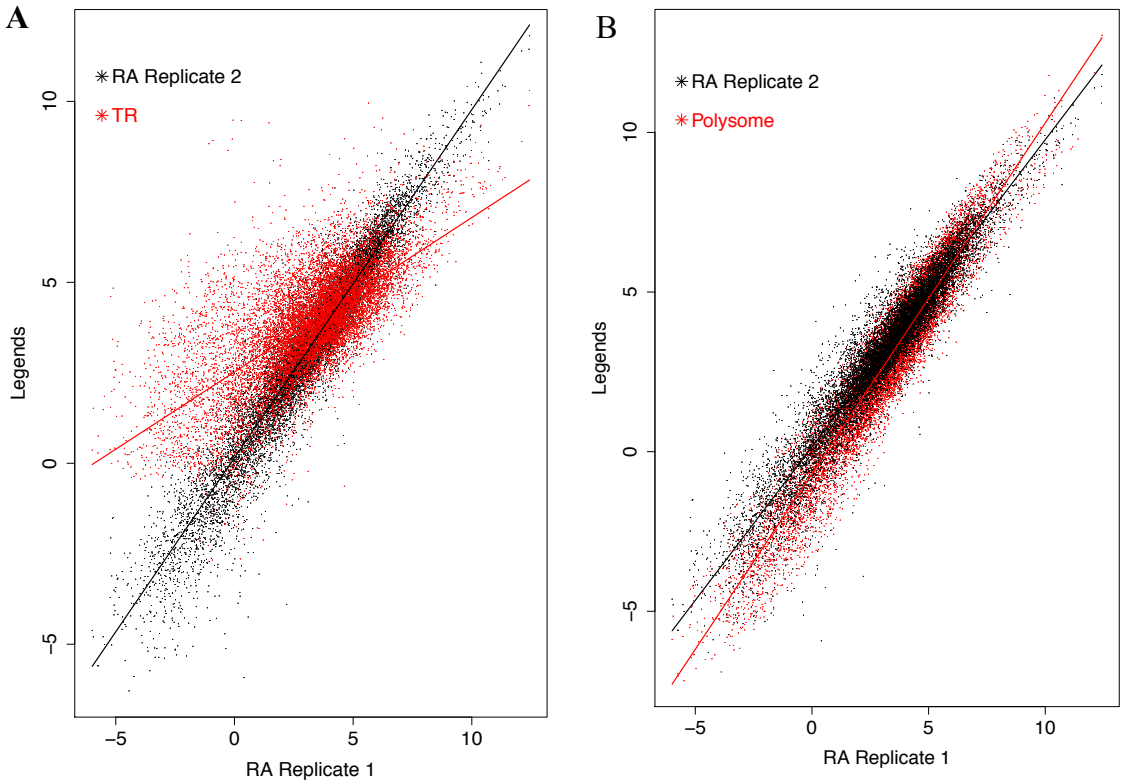

Figure 2: Comparison of TR, RA and TA to illustrate the discrepancy among the three parameters. A. Scatter plot of TR (red) and a RA experimental replicate (black) versus another RA experimental replicate. B. Scatter plot of TA (red) and a RA experimental replicate (black) versus another RA experimental replicate. The same two RA experimental replicates are used in A and B. The linear regression lines are also shown.

for detail). Thus, our approach is able to reveal the inherent differences among the three key transcriptome analysis parameters. We then further dissected the dataset to decipher how the cells coordinate the multiple transcriptome regulatory processes that give rise to the observed discrepancies.

Moderate correlation between mRNA stability and translation activity, and its pathway/function specific pattern

The discrepancy between TR and RA is a reflection of mRNA stability (or the rate of mRNA degradation); a high degradation rate or unstable mRNA leads to lower RA level implicated by the TR – and *vice versa*. Furthermore, it is well known that active translation shields mRNAs from degradation, thus stabilizing the mRNA species and contributing to the discrepancy between TR and RA (Coldwell, Gray et al. 2010). In other words, translation activity should be a major determinant of how RA deviates from TR. Our data provide a unique opportunity, to our knowledge for the first time, for a genome-wide and quantitative assessment of the contribution of this stabilization-by-translation regulatory mechanism to transcriptome regulation. For this purpose, we used the $\log_2$(TA/RA) and $\log_2$(RA/TR) log ratios as translation index and stability index, respectively. The former is the log ratio between actively translated mRNA abundance and total mRNA abundance, thus a measurement of mRNA translation activity normalized against RA; the latter is the log ratio between total mRNA abundance and transcription rate, a measurement of discrepancy between the two parameters.

We hypothesized that the stabilization-by-translation regulatory mechanism should exert a significant effect on the relationship between the two indices. If our hypothesis is wrong, the two indices should be negatively correlated, since RA is the numerator in the stability index and denominator in the translation index. However, our experimental results turned out to be the contrary and, thus, support our hypothesis. As shown in Figure 3A, a dot-plot of the two indices illustrates an overall positive relationship, with a correlation coefficient of 0.39; the linear regression line is also shown to quantify the relationship, with a slope of 0.19. In other words, an overall positive correlation was observed. To illustrate the level of the significance of this observation, we randomized the data by simultaneous permutation of the TR and TA parameters to generate a statistical background model for our analysis. As expected, randomizing the data led to negative correlation coefficients and negative slopes of the linear regression line between the two indexes. We performed the randomization for 1000 times. This generated 1000 correlation

coefficients and 1000 slopes of the corresponding linear regression lines, the boxplots of both of which were shown in Figure 3B. Out of the 1000 randomization, not a single positive correlation was observed – both values were always negative. Figure 3B also shows the experimentally determined positive values of the correlation coefficient and the linear regression line slope, demonstrating a sharp contrast with the respective randomly generated values. This contrast illustrates the magnitude of the difference, i.e., the effect of the stabilization-by-translation regulation mechanism on the relationship between the two indices. Thus, consistent with our hypothesis, the stabilization-by-translation regulatory mechanism renders the relationship into an overall positive one. These results reflect that the higher the proportion of a mRNA species being translated, the lower the proportion that is being degraded. Thus, the dependency of mRNA stability on translation activity, that is, the stabilization-by-translation regulatory mechanism, seems to nicely outline the relationship among transcription rate, mRNA abundance, mRNA stability and translation activity. To put it another way, we were able to delineate the overall relationship among three major transcriptome regulation processes – transcription, mRNA degradation and mRNA translation.

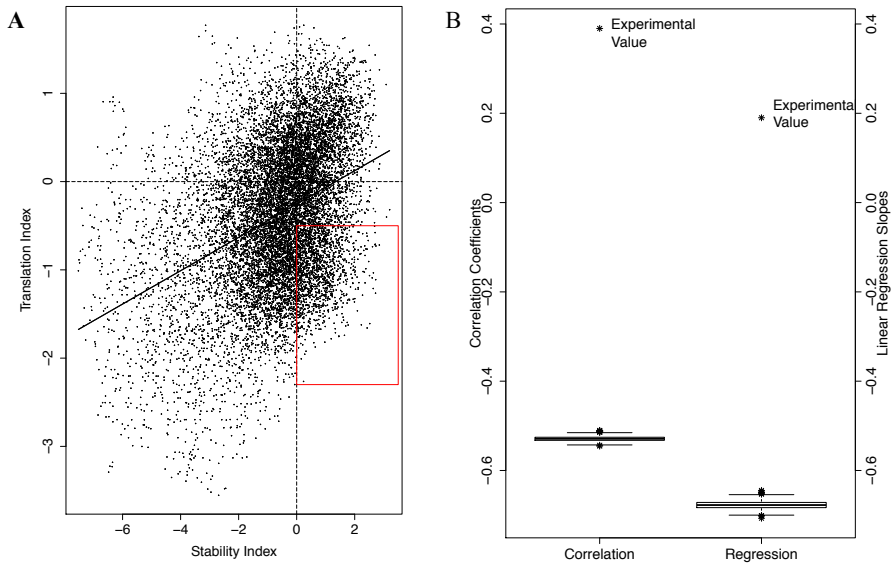

Figure 3: Overall positive correlation between the stability index ($\log_2$(RA/TR)) and the translation index ($\log_2$(TA/RA)). A. Scatter plot of the stability index versus the translation index. The correlation coefficient and the linear regression line between the two indices are also shown. The red rectangle identifies mRNAs with high stability but low translation activity to be further analyzed later (see text and Figure 8). B. Box plot of the correlation coefficient and the slope of linear regression lines between the two indexes upon randomization of the experimental dataset. Values from 1000 randomization were used to generate the boxplot. Experimental values are also shown and denoted.

Nevertheless, the correlation between the two indices, even though statistically significant, is not nearly unequivocal; too many genes deviate significantly from the overall trend – the linear regression line. We asked whether this is due to function specific patterns of gene expression regulation, as genes involved

in the same biological process have been shown to share a similar pattern in other datasets. To answer this question, we performed two systematic analyses. First, we calculated the distances between the coordinates of each gene pair in Figure 3A. We then created the histograms of the pairwise distances between gene pairs associated with similar sets of gene ontology (GO) terms (see Materials and Methods for detail), and also a histogram for the distances between gene pairs with no significant GO similarity. The distance between genes associated with similar GO terms tend to be smaller than those between genes with no significant similarity in their GO association (Figure 4A). The trend is correlated with the GO similarity score; the higher the score, the more the histogram shifts toward short distance range. Second, we performed this comparison of distances between gene pairs whose proteins interact with each other versus gene pairs whose proteins have not been found to interact with each other. This was done with protein-protein interaction data, which was, as we have previously done (Guo, Jiang et al. 2014), downloaded from the IntAct database (Kerrien, Aranda et al. 2012, Orchard, Ammari et al. 2014). As shown in Figure 4B, the interacting pairs exhibit shorter distance than non-interacting pairs. And the trend is correlated with the confidence score assigned to the protein pairs in the IntAct database. Since the protein-protein interaction datasets are generally considered noisy, the confidence score quantify the reliability of the interaction. As shown in Figure 4B, the more reliable the interaction, the more the histogram shifts toward short distance range.

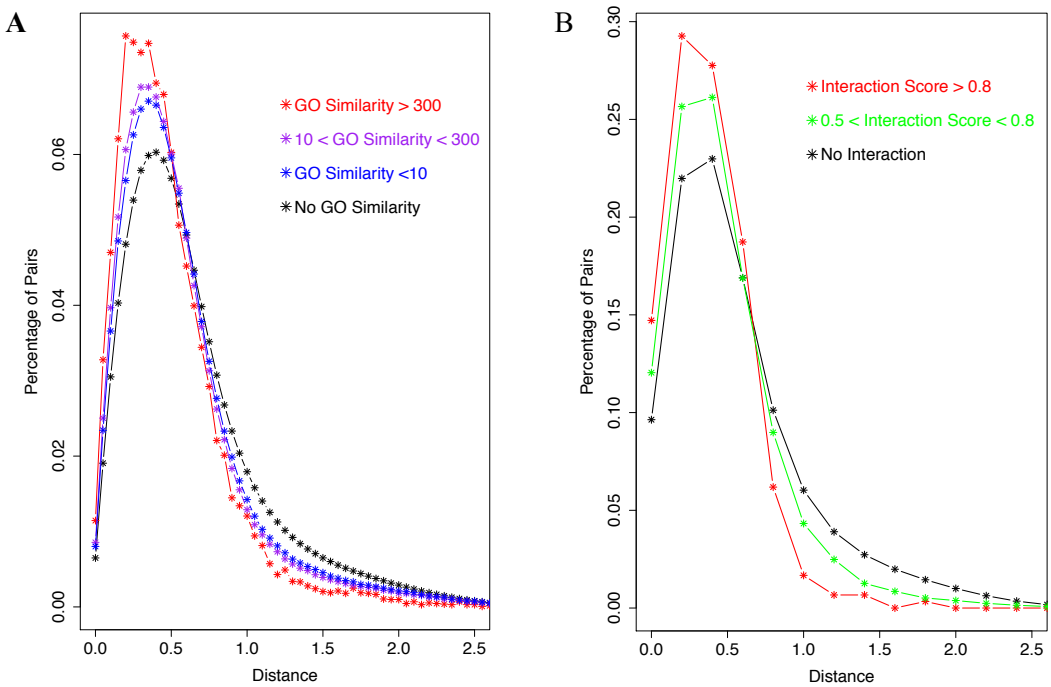

Figure 4: Pathway/function specific pattern of the correlation between the stability and the translation indexes. A. Histograms of the distances between their mRNAs' coordinates in Figure 3A for gene pairs with different levels of GO similarity. B. Histograms of the distances for gene pairs whose proteins were shown to mutually interact with different levels of interaction confidence score.

This function specific pattern is illustrated by the distinct patterns of two exemplary functional groups of genes – the genes for the proteasome subunit (PMS) proteins (PMSA1 to 7 and PMSB1 to 7) and the like-Sm (LSM) genes (LSM1 to 8) (Figure 5). The PMS genes code for proteins that constitute the proteasome 20S core structure (Kish-Trier and Hill 2013). Their mRNAs share a pattern of high levels of both stability and translation activity. The LSM genes code for subunits of two single-stranded-RNA-binding hetero-heptameric ring structures – one cytoplasmic and the other nucleus (Khusial, Plaag et al. 2005). Subunits LSM1 to 7 form the heptamer that is part of the P-body and functions during mRNA degradation in the cytoplasm. Consistently, LSM1-7 mRNAs share a common pattern. However, the pattern is strikingly different from the pattern shared by the PMS mRNAs. While the LSM1-7 mRNA exhibit relatively high stability, unlike PMS mRNA, they exhibit largely lower than average translation activity. The LSM8 subunit interacts with, and nucleus-retains, LSM2 to 7 subunits to form the nucleus heptameric ring structure (Khusial, Plaag et al. 2005). That is, it replaces the LSM1 subunit to form the nucleus heptameric structure. This heptameric structure binds to the U6 snRNA and U8 small nucleolar RNA (snoRNA), and thus functions during general RNA maturation in the nucleus. Consistent with this unique LSM8 function, the LSM8 mRNA does not follow the pattern shared by LSM1 to 7 mRNAs, in that it is relatively unstable (Figure 5).

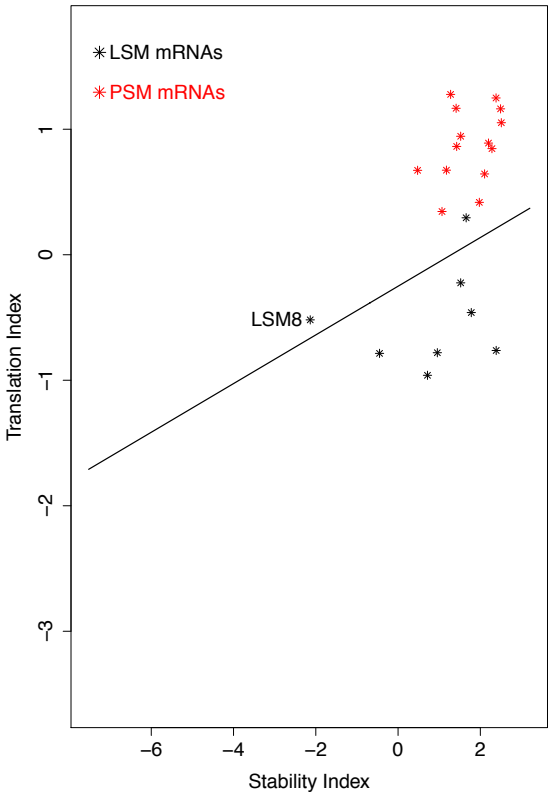

Figure 5: Scatter plot of the stability and the translation indices for mRNAs of the PMS and the LSM functional groups of genes. The PMS mRNAs are shown in red color, and the LSM mRNAs in black color. LSM8 mRNA was denoted.

mRNA UTR proportion is a major determinant of the level of correlation

Next, we tried to gain a mechanistic understanding of this lack of high level of correlation between the translation and the stability indexes, and turned our attention to other post-transcription regulatory mechanisms and the untranslated region (UTR) of mRNAs. Besides the stabilization-by-translation regulation, many other mechanisms exist in multi-cellular eukaryotic species, but have not been accounted for in our analysis. For instance, the miRNAs/siRNAs target and regulate a large portion of the transcriptome. Essentially all regulatory signals for such regulation are embedded in mRNA UTR sequences. Consistently, UTRs are abundant in multi-cellular transcriptomes. This is especially true in human. As shown in Figure 6A, on average, the ORF occupies only ~50% of a human mRNA; the other half is devoted to the UTRs. In many mRNAs, the UTR occupies more than 90% of the total length; for instance, the mRNAs of the all-important CREB1 (cyclic AMP-responsive element-binding protein 1) gene. Since the regulatory signals for mRNA post-transcription regulation are mostly embedded in the UTR sequences, the proportion of an mRNA that is occupied by the UTRs should serve as a good measure of the degree to which the mRNA is controlled by these regulatory mechanisms. Thus, we hypothesized that this proportion should be a major explanatory factor for the lack of a high level correlation between the mRNA stability and translation

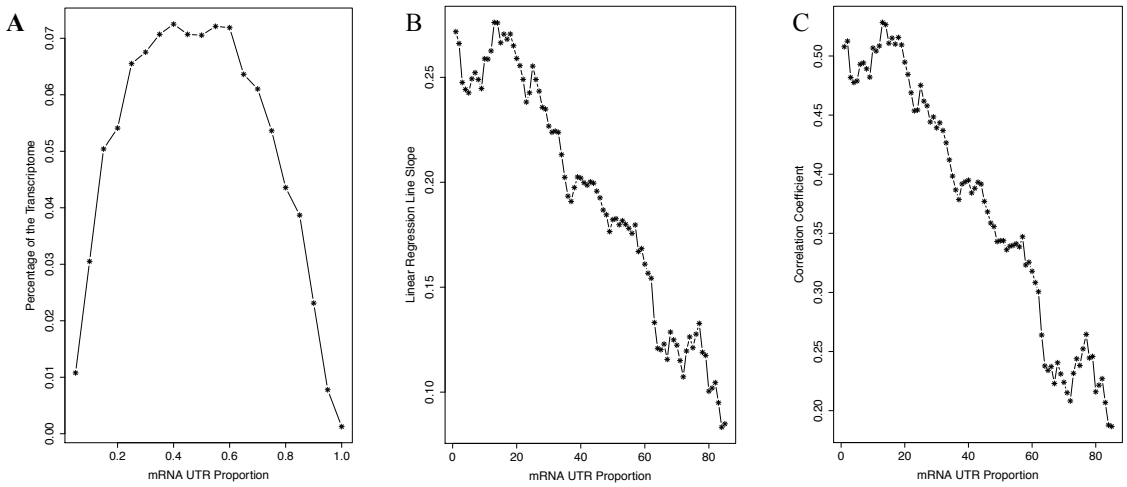

Figure 6: The proportion of a mRNA that is occupied by the UTRs is a determinant of the level of the correlation between the stability and the translation indices. A: Histogram of the UTR proportions of human mRNAs. B and C: The correlation coefficient (B) and the slope of the linear regression line (C) between the stability and the translation indices decrease as the mRNA UTR proportion increases.

indexes. Indeed, our results support this hypothesis. First, the correlation coefficient between the two indices is optimal at ~20% UTR, but steadily decreases as this proportion further increases (Fig. 6B); and so is the slope of the linear regression line between the two indices (Fig. 6C). This is further illustrated by a contrast between mRNAs with ~20% UTRs and those with ~90% UTRs, that is, the higher level of correlation between the two indices for the former and a poor correlation for the latter (Fig. 7). Second, the mRNAs that defy the stabilization-by-translation regulatory mechanism, those that show low translation activity but high stability as identified by the red rectangle in Figure 3A, display higher proportion of UTRs. The histogram of their UTR proportions, when compared with that of the whole transcriptome, shifts toward high proportion ranges.

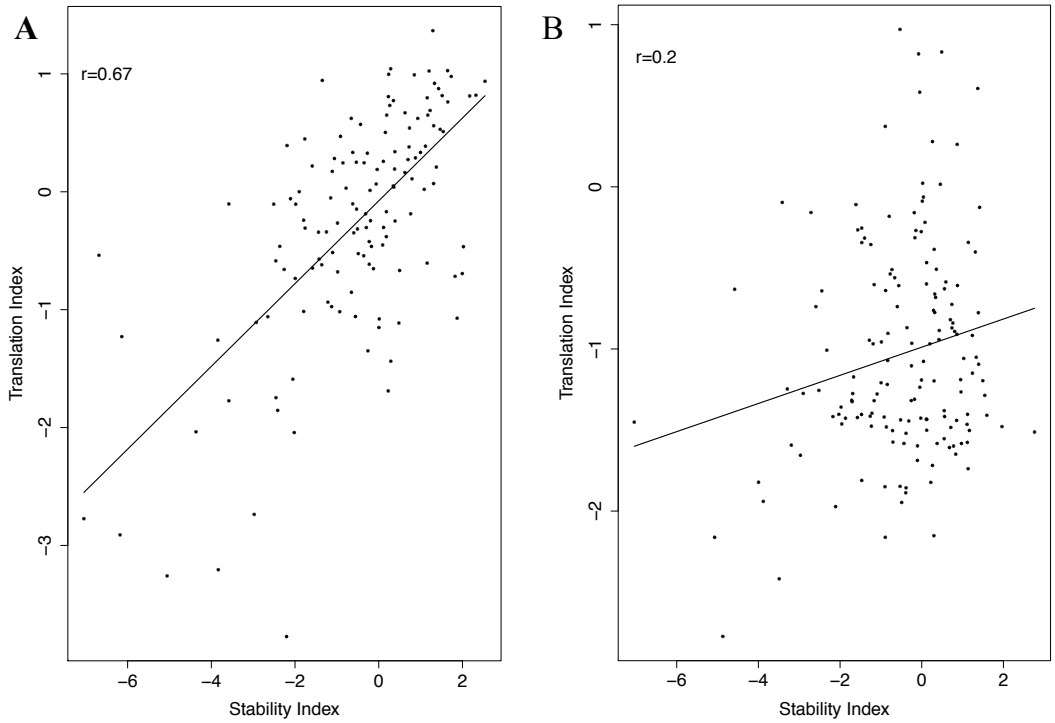

Figure 7. Scatter plots of the stability and the translation indices for mRNAs with a ~20% UTR proportion (A) and those mRNAs with a ~90% UTR proportion (B). The correlation coefficient and the linear regression lines are also shown.

Table 1: Comparison of the UTR proportions of the PSM and the LSM mRNAs			
	No. of Genes	Median	Mean
LSM	8	68.6%	69.6%
PSM	14	26.4%	35.3%
p-value = 0.0004 (two-sample t-test with a "greater than" alternative hypothesis)			

In order to illustrate our observation, we once again used the PMS and the LSM groups of genes shown in Figure 5 (Table 1). The mRNAs of the PMS genes have high levels of both stability and translation activity, and thus exemplify mRNAs controlled by the stabilization-by-translation

mechanism. Consistently, as shown in table 1, they have less-than-average UTR proportions (an average of 35.3% and a median of 26.4%). The mRNAs for the LSM genes, on the other hand, have low levels of translation activity but stay relatively stable, and thus exemplify mRNAs defying the stabilization-by-translation regulatory mechanism. Not surprisingly, they have higher-than-average UTR proportions (a mean of 69.6% and a median of 68.6%). The difference between the UTR proportions of the two groups of mRNAs has, according to a t-test, a significant p-value of 0.0004 (Table 1). Thus, the low quality of the overall correlation between the two indices can be partially explained by post-transcription regulatory mechanisms mediated by mRNA UTRs. To put it another way, multiple regulatory mechanisms control the transcriptome. Multi-parameter approaches, such as ours as shown here, have the urgently needed power to dissect the process and visualize cellular co-ordination of these mechanisms.

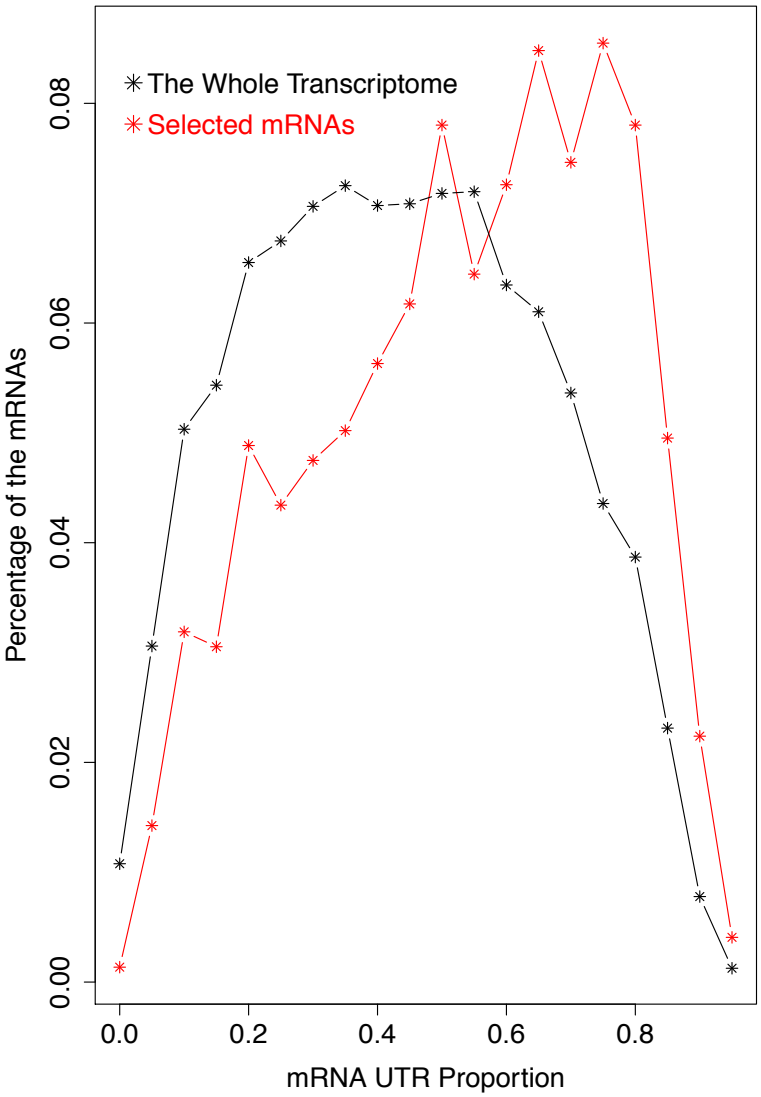

Figure 8: Histogram of the UTR proportions of the mRNAs that have relative high stability but lower-than-average translation activity in comparison with that of the whole human transcriptome. The mRNAs with high stability but low translation activity were selected with the red rectangle in Figure 3A.

Sequentially higher levels of gene expression selectivity from TR to RA, and then to TA

We also set out to explore whether these post-transcription regulations lead to systematic differences among the genomic profiles of the three parameters; that is, whether the consequences of these regulations are manifested in differences in statistical features among the three parameters. As described

earlier and shown in Figure 2, scatter-plotting and linear regression revealed significant differences among the three parameters. Here, we directly compared the statistical features of the genomic profiles of the three parameters. A systematic trend was indeed observed. The levels of dispersion of the three distributions increase from transcription rate to mRNA abundance and then to translation activity (Fig. 9). As a quantification of this trend, the standard deviation increases in the same direction, and the ranges of the distributions also become sequentially larger (Table 2). Consequently, more and more genes display extreme (either low or high) parameter values in this direction. In other words, the gene expression process becomes more and more selective as the genetic information flow in the direction dictated by the Central Dogma.

Table 2: Comparison of the statistical features of the genomic profiles of the three parameters.

	Standard Deviation	Mean	Value Range	
			From	To
$\log_2$(TR)	1.53	3.85	-2.68	10.41
$\log_2$(RA)	2.38	3.18	-6.02	12.33
$\log_2$(TA)	2.77	2.74	-7.18	13.04

Discussion

Regulation of the transcriptome is a major underpinning of cellular operation. It involves, in addition to transcription, many post-transcriptional processes. Multiple parameters, such as TR, RA and mRNA degradation rate, are relevant to this multi-faceted process. Many multi-parameter studies have been reported and revealed significant discrepancies among the parameters, such as those between TR and RA and those between RA and protein abundance, prompting an appreciation for the complexity of transcriptome regulation.

We have previously participated in the study of the complexity of transcriptome regulation, with a desire for a mechanistic understanding of the discrepancies among TR, RA and protein abundance as well as potential operational advantages the cells gain from them. In this study, we took advantages of the power and versatility of NGS analysis through its coupling to traditional experimental protocols. We simultaneously measured three transcriptome regulation parameters: TR, RA and TA. We also indirectly estimate mRNA stability (or degradation rate) by the log ratio of RA and TR ($\log_2$(RA/TR)). Given the importance of mRNA UTRs in post-transcriptional regulation, the data was analyzed in conjunction with individual mRNAs' proportions that are UTRs. To put it another way, we broke open the "blackbox" of

transcriptome regulation and peeked inside for mechanistic insight into how the cells co-ordinate multiple factors that regulate the transcriptome. In the present paper, we publish, to our knowledge, the first genome-wide dataset that enables integrative analysis of TR, RA and TA and mRNA stability.

It is well known that actively translating mRNA are likely protected from degradation, and thus stabilized. In bacteria, this is considered the primary mechanism for mRNA stability regulation. In eukaryotes, more post-transcriptional regulatory mechanisms, such as micro-RNA control, evolutionarily emerged, giving rise to a more complicated scheme of mRNA stability regulation. However, it is certain that the stabilization-by-translation mechanism still play prominent roles in eukaryotic transcriptome regulation. We provide a quantitative analysis of the impact of translation activity on mRNA stability, by showing a moderate but significant positive correlation between mRNA translation and stability indices.

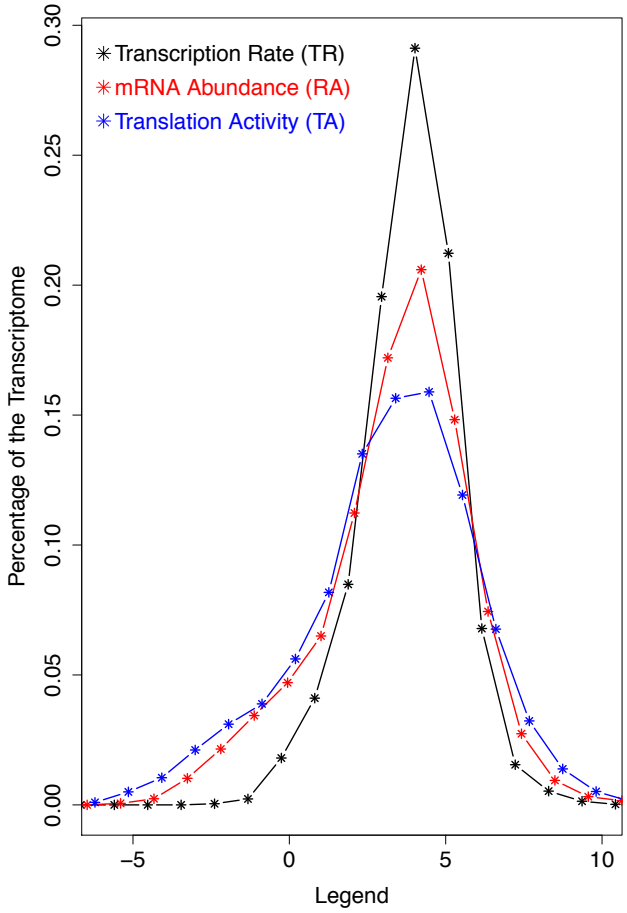

Figure 9: Comparison of the genomic profiles of the three transcriptome parameters – TR, RA and RA. Histograms of TR (black), RA (red) and TA (blue) are shown. The RA and TA histograms are shifted a little bit so that the three histograms have theirs peaks in the same x-axis range, in order to better display the increased levels of dispersion from TR and RA and then to TA.

This correlation between mRNA translation activity and stability has some explanatory power over the discrepancy between TR and RA. High translation activity protects a mRNA species from degradation, while other less translated mRNAs are being actively degraded and removed out of the transcriptome. This leads to enrichment of the mRNA species, resulting in higher steady-state abundance level than that implied by its production rate, *i.e.*, TR. Conversely, low translation activity makes a mRNA species more susceptible to the degradation process, leading to situations where the steady-state abundance level is lower than that implied by the

production rate. The operational advantages the cells gained by implementing this regulatory scheme remain to be elucidated.

Our multi-parameter approach represents a feasible option to enable the much needed systematic analysis of mRNA UTRs. The UTRs are much more abundant in the human transcriptome than in any other transcriptome. Their functions in post-transcriptional regulation are well documented. Essentially, all signals for post-transcriptional regulation reside in the UTRs; for instance, microRNA and siRNA target sites, ARE, IRE-IRP etc. But systematic study of mRNA UTRs has been lacking, and our knowledge about their functions remains fragmentary at best. This is perhaps due to a lack of relevant genomic experimental approaches and datasets. mRNA abundance measurement alone is ill-suited for the study of post-transcription regulatory mechanisms and functional analysis of mRNA UTRs. Additionally, though microRNAs/siRNAs target mRNA UTRs and are major regulators of both translation and mRNA degradation, to our knowledge, microRNA/siRNA study has not been integrated with simultaneous genome-wide measurement of translation activity and mRNA stability. Thus, our integrative multi-parameter analysis represents a novel functional genomic approach to mRNA UTR analysis. It is able to reveal that the UTRs play an important role in maintaining the stability of translationally inactive mRNA species, thus conferring to human cells the capacity for a post-transcriptional regulatory mechanism that is absent in prokaryotic species and mostly in uni-cellular species such as the yeast *S. cerevisiae*. It should be noted that our results represent only a single time-point snap-shot of actively growing human cells. More power of this analysis approach, we believe, is yet to be relished in analyzing dynamic changes of the three parameters during physiological processes.

Additionally, computational analysis of mRNA UTRs for key regulatory signals embedded in the UTR sequences remains technically challenging. This is due to low signal-to-noise ratio and the lack of a general guiding principle. For instance, a typical microRNA target site is no more than 8 nucleotide long. Our approach provides a way to classify the mRNAs based on their patterns in the generated datasets, i.e., their behavior in the multi-faceted transcriptome regulation process. Key regulatory signals shall be shared by the UTRs of similarly classified mRNAs, and thus can be computationally extracted from them – a much easier approach than *de novo* computational analysis of mRNA UTR sequences. That is, datasets generated through this approach should provide a functional context for enhancing the signal-to-noise ratio in computational analysis of mRNA UTR sequences.

We also quantitatively describe the trend of sequentially higher levels of selectivity as the genetic information flow from the genome to the proteome in the gene expression process. In other words, the gene expression machinery focuses its resources on less and less genes, so that only mission critical proteins are expressed in the proteome. The multi-stepped gene expression process can be considered as, to some degree, a selective amplification process. Transcription selectively amplifies the genomic sequences into multiple copies of mRNA sequences. Translation, in turn, selective amplifies individual mRNA molecules into multiple copies of protein sequences. The selectivity of this process is further enhanced by selective mRNA degradation. Even though obvious from the results in previous publications, this trend of sequentially higher levels of selectivity in the gene expression process has not received much attention, and was never explicitly stated in these reports. In this study, we quantitatively described this trend by comparing the dispersions of the genomic profiles of the three gene expression parameters. Our results also suggest that mRNA degradation plays perhaps the biggest role in this trend, as the jump in selectivity from transcription rate to mRNA abundance is much bigger than the increase from mRNA abundance to translation activity. That is, selective degradation of those mRNAs, which are not protected from degradation by active translation or other processes mediated by their UTRs, play an important role in shaping up the transcriptome and priming it for efficient production of mission-critical proteins.

In summary, we present a quantitative delineation of cellular coordination of transcription, mRNA abundance, mRNA stability and mRNA translation activity, as well as mechanistic involvement of mRNA UTRs in the coordination process. As a consequence of the coordination activity, the cells exhibit sequentially higher level of gene expression selectivity from transcription to mRNA abundance, and then to translation activity. The results contribute to our understanding of the complexity of the multi-stepped gene expression process, through which the cells "read" the genomic "book" of seemingly simplistic string of nucleotides and "translate" information embedded in the sequences into cellular operations, that is, dynamic control of the biochemical flow through biochemical reactions, pathways and networks (Searls 1997, Searls 2001, Searls 2002, Wang 2005).

Materials and Methods

Tissue Culture and mRNA Isolation for RNA-seq Analysis

The human HCT116 cells were cultured in a serum-free medium (McCoy's 5A (Sigma) with pyruvate, vitamins, amino acids and antibiotics) supplemented with 10 ng/ml epidermal growth factor, 20 μg/ml insulin and 4 μg/ml transferrin. Cells were maintained at 37 °C in a humidified incubator with 5% CO_2.

To extract mRNA for RNA-seq analysis, RNeasy kit (Qiagen) was used to extract total RNA from the HCT116 cells according to manufacture's specification. GeneRead Pure mRNA Kit (Qiagen) was then used to isolate mRNA from the total RNA for Illumina NGS sequencing according to manufacture's specification.

GRO-seq Analysis

Global run-on was done as previously described (Core, Waterfall et al. 2008, Wang, Garcia-Bassets et al. 2011, Jin, Li et al. 2013). Briefly, two 100cm plates of HCT116 cells were washed 3 times with cold PBS buffer. Cells were then swelled in swelling buffer (10mM Tris-pH7.5, 2mM MgCl2, 3mM CaCl2) for 5min on ice. Harvested cells were re-suspended in 1ml of the lysis buffer (swelling buffer with 0.5% IGEPAL and 10% glycerol) with gentle vortex and brought to 10ml with the same buffer for nuclei extraction. Nuclei were washed with 10ml of lysis buffer and re-suspended in 1ml of freezing buffer (50mM Tris-pH8.3, 40% glycerol, 5mM MgCl2, 0.1mM EDTA), pelleted down again, and finally re-suspended in 100μl of freezing buffer.

For the nuclear run-on step, re-suspended nuclei were mixed with an equal volume of reaction buffer (10mM Tris-pH 8.0, 5mM MgCl2, 1mM DTT, 300mM KCl, 20 units of SUPERase-In, 1% Sarkosyl, 500μM ATP, GTP, and Br-UTP, 2μM CTP) and incubated for 5 min at 30°C. Nuclei RNA were extracted with TRIzol LS reagent (Invitrogen) following manufacturer's instructions, and was resuspended in 20μl of DEPC-water. RNA was then purified through a p-30 RNAse-free spin column (BioRad), according to the manufacturer's instructions and treated with 6.7μl of DNase buffer and 10μl of RQ1 RNase-free DNase (Promega), purified again through a p-30 column. A volume of 8.5μl 10×antarctic phosphatase buffer, 1μl of SUPERase-In, and 5μl of antarctic phosphatase was added to the

run-on RNA and treated for 1hr at 37°C. Before proceeding to immuno-purification, RNA was heated to 65°C for 5min and kept on ice.

Anti-BrdU argarose beads (Santa Cruz Biotech) were blocked in blocking buffer (0.5×SSPE, 1mM EDTA, 0.05% Tween-20, 0.1% PVP, and 1mg/ml BSA) for 1 hr at 4°C. Heated run-on RNA (~85µl) was added to 60µl beads in 500µl binding buffer (0.5×SSPE, 1mM EDTA, 0.05% Tween-20) and allowed to bind for 1hr at 4°C with rotation. After binding, beads were washed once in low salt buffer (0.2×SSPE, 1mM EDTA, 0.05% Tween-20), twice in high salt buffer (0.5% SSPE, 1mM EDTA, 0.05% Tween-20, 150mM NaCl), and twice in TET buffer (TE pH7.4, 0.05% Tween-20). BrdU-incorporated RNA was eluted with 4×125µl elution buffer (20mM DTT, 300mM NaCl, 5mM Tris-pH 7.5, 1mM EDTA, and 0.1% SDS). RNA was then extracted with acidic phenol/chloroform once, chloroform once and precipitated with ethanol overnight. The precipitated RNA was re-suspended in 50µl reaction (45µl of DEPC water, 5.2µl of T4 PNK buffer, 1µl of SUPERase_In and 1µl of T4 PNK (NEB)) and incubated at 37°C for 1 hr. The RNA was extracted and precipitated again as above before being processed for Illumina NGS sequencing.

Polysome Isolation and mRNA extraction

Polysome was isolated as previously described (Feliers, Duraisamy et al. 2005, Day, Cavaglieri Rde et al. 2010). Briefly, the HCT116 cells were incubated with 100µg/ml cycloheximide for 15 minutes, washed three times with PBS, scraped off into PBS, and then pelleted by micro-centrifugation. Cell pellet was homogenized in a hypertonic re-suspension buffer (10 mM Tris (pH 7.5), 250 mM KCl, 2 mM $MgCl_2$ and 0.5% Triton X100) with RNAsin RNAse inhibitor and a protease cocktail. Homogenates were centrifuged for 10 min at 12,000 g to pellet the nuclei. The post-nuclear supernatants were laid on top of a 10-50% (w/v) sucrose gradient, followed by centrifugation for 90 min at 200,000 g. The polysomal fractions were identified by OD_{254} and collected. RNeasy kit (Qiagen) was used to extract RNA from the polysome fractions according to manufacture's specification. GeneRead Pure mRNA Kit (Qiagen) was then used to isolate mRNA for Illumina NGS sequencing from the RNA according to manufacture's specification.

Illumina NGS Sequencing

Sequencing libraries was generated with the Illumina TruSeq RNA Sample Preparation Kit. Briefly, RNA molecules were fragmented into small pieces using divalent cations under elevated temperature. The cleaved RNA fragments are copied into first strand cDNA synthesis using reverse transcriptase and random primers. This was followed by second strand cDNA synthesis using DNA Polymerase I and RNase H. These cDNA fragments were end-repaired using T4 DNA polymerase, Klenow polymerase and T4 polynucleotide kinase. The resulting blunt-ended fragments were A-tailed using a 3′–5′ exonuclease-deficient Klenow fragment and ligated to Illumina adaptor oligonucleotides in a 'TA' ligation. The ligation mixture was further size-selected by AMPure beads and enriched by PCR amplification following Illumina TruSeq DNA Sample Preparation protocol. The resulting library is attached and amplified on a flow-cell by cBot Cluster Generation System.

The sequencing was done with an Illumina HiSeq 2000 sequencer. Multiplexing was used to pool 4 samples into one sequencing lane. After each sequencing run, the raw reads were pro-processed to filter out low quality reads and to remove the multiplexing barcode sequences.

NGS Data Analysis

The sequencing reads were mapped to the UCSC hg19 human genome sequences with the TopHat software, using the default input parameter values. For each sample, at least 80% of the reads were successfully mapped. For the sake of consistence across the three transcriptome regulation parameters, we counted the reads for each gene for the exon regions only. The counting was performed with the HTSeq-count software, and the counts were then transformed into Reads Per Kilo-base Per Million Mapped Reads (RPKM) values. 12921 genes have a minimal RPKM value of 1 for at least one of the three parameters, and were considered expressed in the HCT116 cells.

Statistical Analysis

The R open source statistical software (version 3.3.1) installed on a Mac Pro desktop computer was used for statistical analysis. The student t-test, standard deviation calculation, correlation coefficient calculation, linear regression and other statistical procedure are all done with this R software.

The procedure for comparing the linear regression slopes/coefficients shown in figure 2B is described as follows. We first applied the following linear regression models to the data:

$\log_2(TA) = \mu_1+\beta_1\log2(RA1) + \varepsilon_1$,

$\log_2(RA2) = \mu_2+\beta_2\log2(RA1) + \varepsilon_2$,

and ε_1 and ε_2 follow normal distribution.

It is estimated that

$\widehat{\beta_1}$= 1.11, $\hat{\sigma}(\widehat{\beta_1})$=0.003058, and $\widehat{\beta_1}/\hat{\sigma}(\widehat{\beta_1}) \sim T_{12920}$,

$\widehat{\beta_2} = 0.99, \hat{\sigma}(\widehat{\beta_2}) = 0.001879$ and $\widehat{\beta_2}/\hat{\sigma}(\widehat{\beta_2}) \sim T_{12920}$.

Therefore, the 97.5% confidence interval for β_1 is

$$\beta_1 \pm t_{0.0125,12920}\hat{\sigma}(\widehat{\beta_1}) = (1.101403, 1.115113).$$

The 97.5% confidence interval for β_2 is

$$\beta_2 \pm t_{0.0125,12920}\hat{\sigma}(\widehat{\beta_2}) = (0.9819329, 0.9903571).$$

These two confidence intervals do not overlap, implying that, at significant level 0.05, the two regression coefficients are different.

In addition, because T distribution with degrees of freedom of 12920 is very close to standard normal distribution, the t-score, calculated as below,

$$\widehat{\beta_2} - \widehat{\beta_1} \Big/ \sqrt{\hat{\sigma}^2(\widehat{\beta_2}) + \hat{\sigma}^2(\widehat{\beta_1})}$$

approximately follow standard normal distribution. This allows p-value calculation. The p-value is essentially 0 (smaller than 1E-200).

Gene Ontology (GO) Similarity Analysis

Pairwise GO similarity score between human genes was computed as previously described (Tsoi, Boehnke et al. 2009, Qin, Tsoi et al. 2012, Qin, Matmati et al. 2014). Briefly, for each gene, we first generated GO fingerprint – a set of ontology terms enriched in the PubMed abstracts linked to the gene, along with the adjusted p-value reflecting the degree of enrichment of each term. The GO similarity

score quantifies similarity between the GO fingerprints of corresponding gene pair. For detail about GO fingerprint generation and similarity calculation, please see description in previous publications (Qin, Tsoi et al. 2012).

References

Anders, S., P. T. Pyl and W. Huber (2015). "HTSeq--a Python framework to work with high-throughput sequencing data." Bioinformatics **31**(2): 166-169.

Anderson, L. and J. Seilhamer (1997). "A comparison of selected mRNA and protein abundances in human liver." Electrophoresis **18**(9150937): 533-537.

Brar, G. A., M. Yassour, N. Friedman, A. Regev, N. T. Ingolia and J. S. Weissman (2012). "High-resolution view of the yeast meiotic program revealed by ribosome profiling." Science **335**(6068): 552-557.

Cheng, Z., G. Teo, S. Krueger, T. M. Rock, H. W. Koh, H. Choi and C. Vogel (2016). "Differential dynamics of the mammalian mRNA and protein expression response to misfolding stress." Mol Syst Biol **12**(1): 855.

Coldwell, M. J., N. K. Gray and M. Brook (2010). "Cytoplasmic mRNA: move it, use it or lose it!" Biochem Soc Trans **38**(6): 1495-1499.

Core, L. J., J. J. Waterfall and J. T. Lis (2008). "Nascent RNA sequencing reveals widespread pausing and divergent initiation at human promoters." Science **322**(5909): 1845-1848.

Day, R. T., C. Cavaglieri Rde, H. Tabatabaimir, V. Mantravadi, M. J. Lee, J. L. Barnes, B. S. Kasinath and D. Feliers (2010). "Acute hyperglycemia rapidly stimulates VEGF mRNA translation in the kidney. Role of angiotensin type 2 receptor (AT2)." Cell Signal **22**(12): 1849-1857.

Dolken, L., Z. Ruzsics, B. Radle, C. C. Friedel, R. Zimmer, J. Mages, R. Hoffmann, P. Dickinson, T. Forster, P. Ghazal and U. H. Koszinowski (2008). "High-resolution gene expression profiling for simultaneous kinetic parameter analysis of RNA synthesis and decay." RNA **14**(9): 1959-1972.

Eser, P., C. Demel, K. C. Maier, B. Schwalb, N. Pirkl, D. E. Martin, P. Cramer and A. Tresch (2014). "Periodic mRNA synthesis and degradation co-operate during cell cycle gene expression." Mol Syst Biol **10**: 717.

Feliers, D., S. Duraisamy, J. L. Barnes, G. Ghosh-Choudhury and B. S. Kasinath (2005). "Translational regulation of vascular endothelial growth factor expression in renal epithelial cells by angiotensin II." Am J Physiol Renal Physiol **288**(3): F521-529.

Flory, M. R., H. Lee, R. Bonneau, P. Mallick, K. Serikawa, D. R. Morris and R. Aebersold (2006). "Quantitative proteomic analysis of the budding yeast cell cycle using acid-cleavable isotope-coded affinity tag reagents." Proteomics **6**(17133367): 6146-6157.

Friedel, C. C., L. Dolken, Z. Ruzsics, U. H. Koszinowski and R. Zimmer (2009). "Conserved principles of mammalian transcriptional regulation revealed by RNA half-life." Nucleic Acids Res **37**(17): e115.

Garcia-Martinez, J., A. Aranda and J. E. Perez-Ortin (2004). "Genomic run-on evaluates transcription rates for all yeast genes and identifies gene regulatory mechanisms." Mol Cell **15**(15260981): 303-313.

Ghaemmaghami, S., W. K. Huh, K. Bower, R. W. Howson, A. Belle, N. Dephoure, E. K. O'Shea and J. S. Weissman (2003). "Global analysis of protein expression in yeast." Nature **425**(6959): 737-741.

Goodwin, S., J. D. McPherson and W. R. McCombie (2016). "Coming of age: ten years of next-generation sequencing technologies." Nat Rev Genet **17**(6): 333-351.

Greenbaum, D., C. Colangelo, K. Williams and M. Gerstein (2003). "Comparing protein abundance and mRNA expression levels on a genomic scale." Genome Biol **4**(12952525): 117-117.

Griffin, T. J., S. P. Gygi, T. Ideker, B. Rist, J. Eng, L. Hood and R. Aebersold (2002). "Complementary profiling of gene expression at the transcriptome and proteome levels in Saccharomyces cerevisiae." Molecular & cellular proteomics : MCP **1**(4): 323-333.
Guo, Z., W. Jiang, N. Lages, W. Borcherds and D. Wang (2014). "Relationship between gene duplicability and diversifiability in the topology of biochemical networks." BMC Genomics **15**: 577.
Gygi, S. P., Y. Rochon, B. R. Franza and R. Aebersold (1999). "Correlation between protein and mRNA abundance in yeast." Mol Cell Biol **19**(10022859): 1720-1730.
Hah, N., C. G. Danko, L. Core, J. J. Waterfall, A. Siepel, J. T. Lis and W. L. Kraus (2011). "A rapid, extensive, and transient transcriptional response to estrogen signaling in breast cancer cells." Cell **145**(4): 622-634.
Hayles, B., S. Yellaboina and D. Wang (2010). "Comparing transcription rate and mRNA abundance as parameters for biochemical pathway and network analysis." PloS one **5**(3): e9908.
Ideker, T., V. Thorsson, J. A. Ranish, R. Christmas, J. Buhler, J. K. Eng, R. Bumgarner, D. R. Goodlett, R. Aebersold and L. Hood (2001). "Integrated genomic and proteomic analyses of a systematically perturbed metabolic network." Science **292**(11340206): 929-934.
Ingolia, N. T., S. Ghaemmaghami, J. R. Newman and J. S. Weissman (2009). "Genome-wide analysis in vivo of translation with nucleotide resolution using ribosome profiling." Science **324**(5924): 218-223.
Jin, F., Y. Li, J. R. Dixon, S. Selvaraj, Z. Ye, A. Y. Lee, C. A. Yen, A. D. Schmitt, C. A. Espinoza and B. Ren (2013). "A high-resolution map of the three-dimensional chromatin interactome in human cells." Nature **503**(7475): 290-294.
Jovanovic, M., M. S. Rooney, P. Mertins, D. Przybylski, N. Chevrier, R. Satija, E. H. Rodriguez, A. P. Fields, S. Schwartz, R. Raychowdhury, M. R. Mumbach, T. Eisenhaure, M. Rabani, D. Gennert, D. Lu, T. Delorey, J. S. Weissman, S. A. Carr, N. Hacohen and A. Regev (2015). "Immunogenetics. Dynamic profiling of the protein life cycle in response to pathogens." Science **347**(6226): 1259038.
Kerrien, S., B. Aranda, L. Breuza, A. Bridge, F. Broackes-Carter, C. Chen, M. Duesbury, M. Dumousseau, M. Feuermann, U. Hinz, C. Jandrasits, R. C. Jimenez, J. Khadake, U. Mahadevan, P. Masson, I. Pedruzzi, E. Pfeiffenberger, P. Porras, A. Raghunath, B. Roechert, S. Orchard and H. Hermjakob (2012). "The IntAct molecular interaction database in 2012." Nucleic acids research **40**(Database issue): D841-846.
Khusial, P., R. Plaag and G. W. Zieve (2005). "LSm proteins form heptameric rings that bind to RNA via repeating motifs." Trends Biochem Sci **30**(9): 522-528.
Kim, D., G. Pertea, C. Trapnell, H. Pimentel, R. Kelley and S. L. Salzberg (2013). "TopHat2: accurate alignment of transcriptomes in the presence of insertions, deletions and gene fusions." Genome Biol **14**(4): R36.
Kish-Trier, E. and C. P. Hill (2013). "Structural biology of the proteasome." Annu Rev Biophys **42**: 29-49.
Le Roch, K. G., J. R. Johnson, L. Florens, Y. Zhou, A. Santrosyan, M. Grainger, S. F. Yan, K. C. Williamson, A. A. Holder, D. J. Carucci, J. R. Yates, 3rd and E. A. Winzeler (2004). "Global analysis of transcript and protein levels across the Plasmodium falciparum life cycle." Genome Res **14**(11): 2308-2318.
Li, J. J., P. J. Bickel and M. D. Biggin (2014). "System wide analyses have underestimated protein abundances and the importance of transcription in mammals." PeerJ **2**: e270.
Liu, Y. and R. Aebersold (2016). "The interdependence of transcript and protein abundance: new data--new complexities." Mol Syst Biol **12**(1): 856.

Marin-Navarro, J., A. Jauhiainen, J. Moreno, P. Alepuz, J. E. Perez-Ortin and P. Sunnerhagen (2011). "Global estimation of mRNA stability in yeast." Methods Mol Biol **734**: 3-23.
McManus, J., Z. Cheng and C. Vogel (2015). "Next-generation analysis of gene expression regulation--comparing the roles of synthesis and degradation." Mol Biosyst **11**(10): 2680-2689.
Molina-Navarro, M. M., L. Castells-Roca, G. Belli, J. Garcia-Martinez, J. Marin-Navarro, J. Moreno, J. E. Perez-Ortin and E. Herrero (2008). "Comprehensive transcriptional analysis of the oxidative response in yeast." J Biol Chem **283**(18424442): 17908-17918.
Morozov, I. Y., M. G. Jones, P. D. Gould, V. Crome, J. B. Wilson, A. J. Hall, D. J. Rigden and M. X. Caddick (2012). "mRNA 3' tagging is induced by nonsense-mediated decay and promotes ribosome dissociation." Mol Cell Biol **32**(13): 2585-2595.
Orchard, S., M. Ammari, B. Aranda, L. Breuza, L. Briganti, F. Broackes-Carter, N. H. Campbell, G. Chavali, C. Chen, N. del-Toro, M. Duesbury, M. Dumousseau, E. Galeota, U. Hinz, M. Iannuccelli, S. Jagannathan, R. Jimenez, J. Khadake, A. Lagreid, L. Licata, R. C. Lovering, B. Meldal, A. N. Melidoni, M. Milagros, D. Peluso, L. Perfetto, P. Porras, A. Raghunath, S. Ricard-Blum, B. Roechert, A. Stutz, M. Tognolli, K. van Roey, G. Cesareni and H. Hermjakob (2014). "The MIntAct project--IntAct as a common curation platform for 11 molecular interaction databases." Nucleic Acids Res **42**(Database issue): D358-363.
Qin, T., N. Matmati, L. C. Tsoi, B. K. Mohanty, N. Gao, J. Tang, A. B. Lawson, Y. A. Hannun and W. J. Zheng (2014). "Finding pathway-modulating genes from a novel Ontology Fingerprint-derived gene network." Nucleic Acids Res **42**(18): e138.
Qin, T., L. C. Tsoi, K. J. Sims, X. Lu and W. J. Zheng (2012). "Signaling network prediction by the Ontology Fingerprint enhanced Bayesian network." BMC Syst Biol **6 Suppl 3**: S3.
Rabani, M., J. Z. Levin, L. Fan, X. Adiconis, R. Raychowdhury, M. Garber, A. Gnirke, C. Nusbaum, N. Hacohen, N. Friedman, I. Amit and A. Regev (2011). "Metabolic labeling of RNA uncovers principles of RNA production and degradation dynamics in mammalian cells." Nat Biotechnol **29**(5): 436-442.
Rabani, M., R. Raychowdhury, M. Jovanovic, M. Rooney, D. J. Stumpo, A. Pauli, N. Hacohen, A. F. Schier, P. J. Blackshear, N. Friedman, I. Amit and A. Regev (2014). "High-resolution sequencing and modeling identifies distinct dynamic RNA regulatory strategies." Cell **159**(7): 1698-1710.
Romero-Santacreu, L., J. Moreno, J. E. Perez-Ortin and P. Alepuz (2009). "Specific and global regulation of mRNA stability during osmotic stress in Saccharomyces cerevisiae." RNA **15**(19369426): 1110-1120.
Schwanhausser, B., D. Busse, N. Li, G. Dittmar, J. Schuchhardt, J. Wolf, W. Chen and M. Selbach (2011). "Global quantification of mammalian gene expression control." Nature **473**(7347): 337-342.
Searls, D. B. (1997). "Linguistic approaches to biological sequences." Comput Appl Biosci **13**(9283748): 333-344.
Searls, D. B. (2001). "Reading the book of life." Bioinformatics **17**(7): 579-580.
Searls, D. B. (2002). "The language of genes." Nature **420**(12432405): 211-217.
Tian, Q., S. B. Stepaniants, M. Mao, L. Weng, M. C. Feetham, M. J. Doyle, E. C. Yi, H. Dai, V. Thorsson, J. Eng, D. Goodlett, J. P. Berger, B. Gunter, P. S. Linseley, R. B. Stoughton, R. Aebersold, S. J. Collins, W. A. Hanlon and L. E. Hood (2004). "Integrated genomic and proteomic analyses of gene expression in Mammalian cells." Mol Cell Proteomics **3**(10): 960-969.
Tsoi, L. C., M. Boehnke, R. L. Klein and W. J. Zheng (2009). "Evaluation of genome-wide association study results through development of ontology fingerprints." Bioinformatics **25**(10): 1314-1320.

Vogel, C. and E. M. Marcotte (2012). "Insights into the regulation of protein abundance from proteomic and transcriptomic analyses." Nat Rev Genet **13**(4): 227-232.
Wang, D. (2008). "Discrepancy between mRNA and protein abundance: insight from information retrieval process in computers." Computational biology and chemistry **32**(6): 462-468.
Wang, D., I. Garcia-Bassets, C. Benner, W. Li, X. Su, Y. Zhou, J. Qiu, W. Liu, M. U. Kaikkonen, K. A. Ohgi, C. K. Glass, M. G. Rosenfeld and X. D. Fu (2011). "Reprogramming transcription by distinct classes of enhancers functionally defined by eRNA." Nature **474**(7351): 390-394.
Wang, D. G. (2005). ""Molecular gene": Interpretation in the right context." Biology & Philosophy **20**(2-3): 453-464.
Washburn, M. P., A. Koller, G. Oshiro, R. R. Ulaszek, D. Plouffe, C. Deciu, E. Winzeler and J. R. Yates (2003). "Protein pathway and complex clustering of correlated mRNA and protein expression analyses in Saccharomyces cerevisiae." Proc Natl Acad Sci U S A **100**(12626741): 3107-3112.